Microstructural Evolution of Ultrathin Amorphous Silicon Films by Real-Time Spectroscopic Ellipsometry

Ilsin An, H. V. Nguyen, N. V. Nguyen, and R. W. Collins
Materials Research Laboratory and The Department of Physics, The Pennsylvania State University, University Park, Pennsylvania 16802
(Received 12 July 1990)

The nucleation of thin-film amorphous silicon (*a*-Si), sputter deposited on oxidized *c*-Si, is investigated by real-time spectroscopic ellipsometry from 1.5 to 4.5 eV with a resolution of 3 s and a repetition period of 15 s. Analysis of real-time spectra provides unprecedented sensitivity and quantitative information on the microstructural evolution. Under preparation conditions resulting in *a*-Si of the highest bulk Si-Si bond-packing density, an abrupt transition representing the onset of bulk film growth can be identified unambiguously when nuclei reach a thickness of 13 ± 1 Å.

PACS numbers: 68.55.Jk, 07.60.Fs, 78.65.Gb, 81.15.Cd

Thin films prepared by vapor deposition have numerous applications which demand precise control over microstructural, electronic, and optical properties. Empirical classification schemes for thin-film morphology have been developed to provide insights into relationships between the preparation parameters and resulting properties.[1-3] Continuum,[4] molecular-dynamics,[5] Monte Carlo,[6] and ballistic aggregation[7] computational techniques have also been applied to model film growth and to elucidate the physical principles that underlie the observed morphological development.

In early studies of amorphous Si (*a*-Si), microstructural features as small as 10 Å have been revealed in relatively thick (> 100 Å), porous films by electron microscopy,[8,9] but reports of nucleation-related morphology in ultrathin films are not available owing to inadequate sensitivity. Scanning tunneling microscopy can provide such information, but is difficult to perform on poorly conducting *a*-Si.[10] In any event, real-time probes capable of application in adverse environments are desirable in order to deduce continuous, quantitative information and to make connection with film-growth simulations. Motivated by this goal, real-time spectroscopic ellipsometry (SE) from the near infrared to near ultraviolet has been developed.[11]

We have chosen pure *a*-Si for our first study of thin-film nucleation for a number of reasons. (1) The Bruggeman effective-medium approximation has been applied successfully to calculate the dielectric function of density-deficient *a*-Si, using mixtures of dense material and void.[12] (2) Dielectric functions from a number of laboratories agree closely once bond-packing density variations are considered.[13] (3) Size effects which influence the optical functions of crystalline thin films are expected to be small for *a*-Si. (4) Amorphous films grow uniformly in comparison to polycrystalline or microcrystalline materials as demonstrated by single-photon-energy ellipsometry[14] and electron microscopy of multilayers.[15] Thus, our experimental sensitivity is pushed to the limit, in a situation where conventional probes have failed to detect nucleation.

Single-photon-energy ellipsometry has been used extensively to study *a*-Si(:H) growth[14,16,17] but the data are often difficult to interpret. A geometrical model is usually assumed, and fits to the pseudodielectric function trajectory, swept out as a function of time during film growth, provide model parameters such as the initial nuclei spacing. There is no redundant information available to check the uniqueness of the model. In a spectroscopic measurement, however, each full pair of pseudodielectric function spectra can be interpreted independently by linear regression analysis (LRA) to deduce photon-energy-independent structural parameters, void volume fractions and thicknesses, and their confidence limits.[18] Thus, uniqueness can be assessed and geometrical information can be established *a posteriori*.

In this study, *a*-Si was dc magnetron sputtered onto *c*-Si substrates with intact 20–25-Å native oxides. The target-substrate spacing was 13.9 cm, and the base pressure was 1.3×10^{-6} Pa. For films with the highest Si-Si bond-packing density, the substrate temperature and operating Ar pressure were 300 °C and 6.7×10^{-2} Pa. The sputtering power could be varied from 5 to 50 W, resulting in time-averaged deposition rates from 1.83 to 9.16 Å/min, without influencing the nucleation features discussed below. The film is optically accessible through chamber windows, aligned for a 70° angle of incidence.

Real-time data were collected with a rotating-polarizer-type ellipsometer which employs multichannel detection for a 1.49–4.64-eV spectral range.[11] A 116-point pair of spectra, $\{\psi(h\nu),\Delta(h\nu)\}$, can be obtained in 40 ms, corresponding to an optical period. Here ψ and Δ are given by $r_p/r_s \equiv \tan\psi \exp(i\Delta)$, where r_p and r_s are the complex amplitude reflection coefficients.[19] To improve the signal-to-noise ratio and achieve monolayer sensitivity, eighty periods were averaged for an acquisition time of 3.2 s. In this time, the average *a*-Si accumulation is 0.098 Å at 5 W. Complete $\{\psi(h\nu),\Delta(h\nu)\}$ were obtained every 14.5 s, corresponding to 0.44 Å at 5 W.

Figure 1 shows raw pseudodielectric function data,

© 1990 The American Physical Society

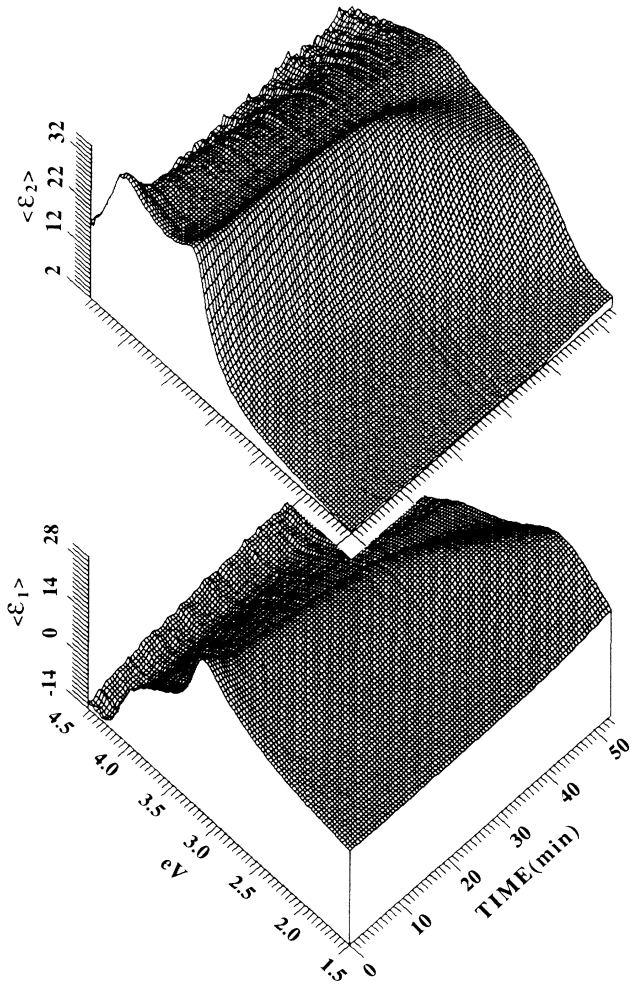

FIG. 1. Pseudodielectric function obtained during the growth of a-Si on c-Si.

$\{\langle\varepsilon_1(h\nu)\rangle,\langle\varepsilon_2(h\nu)\rangle\}$, for a-Si growth at 300 °C, 6.7 $\times 10^{-2}$ Pa, and 5 W, calculated from $\{\psi(h\nu),\Delta(h\nu)\}$ using the Fresnel equations for a single interface.[19] The actual dielectric function for bulk a-Si at 300 °C must be determined in order to apply LRA to the raw data and deduce photon-energy-independent parameters that characterize the morphological development.[18] As a result, another film was prepared under conditions that maximize Si-Si bond-packing density, was cooled from its deposition temperature to 25 °C, and measured. The results were interpreted by LRA using the well-known a-Si dielectric function at 25 °C,[13] applying a two-layer (roughness/bulk) model with variable Si-Si bond-packing densities for the layers (relative to the reference). From the deduced thicknesses and the surface-layer bond-packing density, $\{\langle\varepsilon_1(h\nu)\rangle,\langle\varepsilon_2(h\nu)\rangle\}$ at 300 °C were inverted to obtain the desired bulk dielectric function.

We applied the 300 °C bulk dielectric function in one-layer and two-layer models for the a-Si film of Fig. 1 in order to interpret $\{\langle\varepsilon_1(h\nu)\rangle,\langle\varepsilon_2(h\nu)\rangle\}$ in the first 30

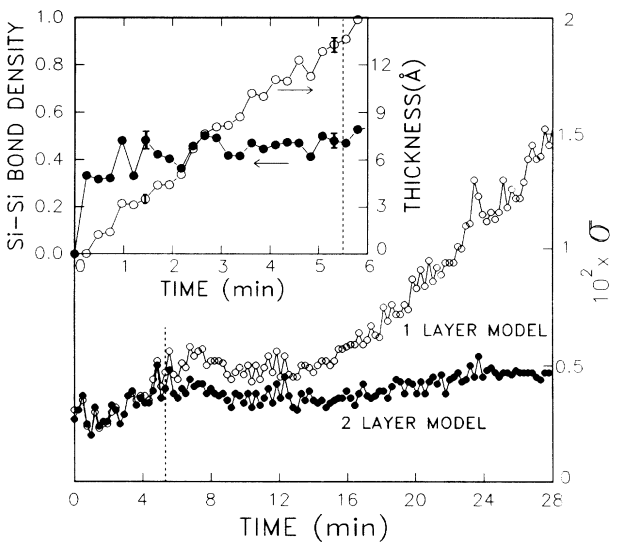

FIG. 2. Unbiased estimator of the mean-square deviation σ obtained in a LRA fit of the data of Fig. 1 for one-layer and two-layer (roughness/bulk) models. Inset: Parameters obtained from the one-layer model, appropriate for times less than the vertical lines. Error bars denote selected 90%-confidence limits.

min. For the one-layer model, the free parameters were the a-Si film thickness and the Si-Si bond-packing density (relative to the bulk). The initial two-layer model simulated a (surface roughness)/(bulk) structure with three independent parameters, the roughness and bulk layer thicknesses and the roughness-layer bond-packing density. Because a nearly constant value of 0.47 was obtained versus time for the latter, it was fixed in subsequent analyses. Figure 2 provides a measure of the quality (σ) of the LRA best fits for the two models.[18] For times greater than ~5–6 min inclusion of the second layer provides a definite improvement, whereas for earlier times the data cannot support a two-layer model. The low σ value throughout the data set attests to the validity of a simple model which includes a transition from one to two layers.

The inset in Fig. 2 depicts the parameters of the one-layer model in the first 6 min. The substrate coverage in the first monolayer is ~40%, and a weak linear densification trend occurs in the first 15 Å. The results for thickness over this range imply a linear increase in deposited mass versus time. Figure 3 includes the two-layer model parameters over the ~30-min deposition time. An abrupt transition in the growth of the low-density layer is evident at 5.5 min. Before the transition, this layer is rapidly increasing and is identical in thickness (within ± 0.2 Å) to the nucleating film in Fig. 2 (inset). After 5.5 min, this layer is only gradually increasing, and represents a true surface layer atop the bulk film. The transition from nuclei growth to bulk film growth occurs over an interval of < 1.5 min or < 3 Å. At the transition, the bulk film is 2.5 Å, which is inter-

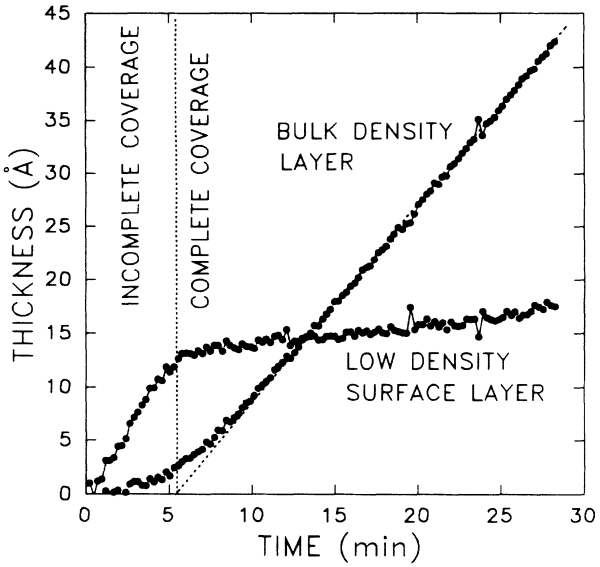

FIG. 3. Evolution of a-Si surface roughness and bulk layer thicknesses for the deposition and two-layer model of Figs. 1 and 2. The 90%-confidence limits are smaller than the radii of the data points.

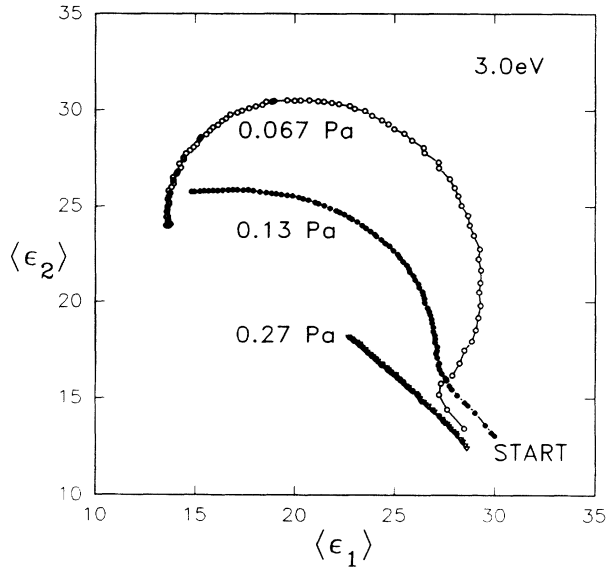

FIG. 4. Pseudodielectric function trajectories at 3.0 eV for a-Si depositions (300 °C, 50 W) at different Ar pressures. Mean free paths for Ar at room temperature range from 11 to 3 cm for pressures from 0.067 to 0.27 Pa.

preted as the monolayer thickness; below the transition, the bulk film is unphysical, being submonolayer. Therefore the conclusion of Fig. 2 is corroborated: The two-layer model is an overinterpretation of the data for $t < 5.5$ min. After ~8–9 min the bulk film thickness is a linear function of time, extrapolating to zero at the transition (broken line). All these features have been observed reproducibly in two other depositions at 50 W.

The slope discontinuity in Fig. 3 indicates that the transition to bulk film growth occurs over a thickness increase of just one monolayer, suggesting abrupt densification when nuclei reach a critical thickness of 13 Å. Just prior to complete coverage, the average bond-packing density through the film is ~50%. We do not call this phenomenon "coalescence" because the earliest growth morphology remains on the film surface and does not decay when the bulk a-Si monolayer is completed. If the in-plane and out-of-plane scales of the initial growth clusters are roughly equal, then continuum models of film growth[20] would suggest a surface diffusion length of < 13 Å for Si precursors on a-Si because the surface roughness after the transition gradually increases in thickness (see Fig. 3; $t > 5.5$ min).

For a-Si:H prepared on c-Si at 250 °C by plasma chemical-vapor deposition (CVD) from SiH_4, single-photon-energy ellipsometry has revealed an abrupt feature in the pseudodielectric function trajectory,[14] but it was difficult to ascribe it uniquely to a specific microstructural event. Surface smoothening was proposed, and the overall results suggested that morphology induced by 40–50-Å nuclei decay to a 6-Å surface roughness layer—true coalescence behavior.[21] A surface diffusion length of ~80 Å was estimated from these results. Two possible models explain the differences in nucleation scale for sputtered a-Si and plasma CVD a-Si:H. Within a homogeneous nucleation model, the higher surface diffusion length in plasma CVD may lead to a lower density of critical-size nuclei. Within a heterogeneous model, the higher impact energy in sputtering may generate a higher density of nucleation sites. Further work is required to distinguish between these possibilities.

The data of Figs. 2 (inset) and 3 can be converted to mass thickness, or the thickness of the equivalent mass of bulk a-Si, versus time. The results indicate that the rate of mass thickness increase is 28% less during nucleation than after bulk film growth. From a coverage factor of ~40%, we find that the effective sticking coefficient of impinging Si on the native SiO_2 is at least 50% less than that on a-Si. Presumably this leads to clustering on an in-plane scale greater than the Si diffusion length on a-Si and to an eventual enhancement of the microstructure.

Results for depositions at 300 ± 5 °C and 50 W under different Ar pressures, presented in Fig. 4 as 3.0-eV trajectories, demonstrate that the formation of the full-coverage, bulk a-Si layer in the early growth stages is driven by adatom surface mobility. Analysis of the lowest-pressure data gives behavior identical to that in Figs. 2 and 3 despite a higher deposition rate. The abrupt slope change in the 0.067-Pa trajectory at $(\langle\varepsilon_1\rangle,\langle\varepsilon_2\rangle) = (27,15)$ identifies the transition to bulk film growth. In analyzing the full spectra for the two higher pressures, we found that the two-layer σ increases well above its initial value over time, showing that a bulk density monolayer is never generated and that the film bond-packing density is graded without a sharp interface

between surface and bulk layers. It is clear then that the columnar film morphology well documented in the classification schemes[2] originates from microstructure developed within the first atomic layers.

To summarize, real-time spectroscopic ellipsometry from 1.5 to 4.5 eV has been applied for quantitative analysis of sputtered *a*-Si film microstructure in the initial nucleation stage. For deposition conditions that lead to material of the highest Si-Si bond-packing density, an abrupt transition from the growth of nuclei to the growth of a bulk film occurs after the nuclei reach 13 Å. The transition is observed in three features of the data analysis, which was performed using one- and two-layer models. This transition reflects the formation of a bulk monolayer at the substrate interface and is not observed when the incident species are thermalized and impact the substrate at lower energies.

The authors are grateful to H. Witham and Professor K. Vedam and Professor R. Messier for their contributions to real-time spectroscopic ellipsometry. Helpful discussions with Professor J. S. Lannin and Dr. B.-Y. Yang are appreciated. We acknowledge support from the National Science Foundation (Grants No. DMR-8901031 and No. DMR-8957159), from Philips-DuPont Optical (H.V.N.), and from the State of Pennsylvania, Ben Franklin Program (N.V.N.).

[1]B. A. Movchan and A. V. Demchishin, Fiz. Met. Metalloved. **28**, 653 (1969) [Phys. Met. Metallogr. **28**, 83 (1969)].

[2]J. A. Thornton, Annu. Rev. Mater. Sci. **7**, 239 (1977).

[3]R. Messier, A. P. Giri, and R. A. Roy, J. Vac. Sci. Technol. A **2**, 500 (1984).

[4]S. Lichter and J. Chen, Phys. Rev. Lett. **56**, 1396 (1986).

[5]H. J. Leamy, G. H. Gilmer, and A. G. Dirks, in *Current Topics in Material Science,* edited by E. Kaldis (North-Holland, Amsterdam, 1980), p. 309.

[6]B. Lewis and J. C. Anderson, *Nucleation and Growth of Thin Films* (Academic, New York, 1978), p. 206.

[7]H. J. Leamy and A. G. Dirks, Appl. Phys. Lett. **25**, 641 (1978).

[8]J. C. Knights and R. A. Lujan, Appl. Phys. Lett. **35**, 244 (1979).

[9]R. Messier and R. C. Ross, J. Appl. Phys. **53**, 6220 (1982).

[10]R. Wiesendanger *et al.*, J. Appl. Phys. **63**, 4515 (1988).

[11]Y.-T. Kim, K. Vedam, and R. W. Collins, Surf. Sci. (to be published).

[12]D. E. Aspnes, J. B. Theeten, and F. Hottier, Phys. Rev. B **20**, 3292 (1979).

[13]D. E. Aspnes, A. A. Studna, and E. Kinsbron, Phys. Rev. B **29**, 768 (1984).

[14]R. W. Collins, in *Amorphous Silicon and Related Materials,* edited by H. Fritzsche (World Scientific, Singapore, 1988), p. 1003.

[15]H. Deckman, J. H. Dunsmuir, and B. Abeles, Appl. Phys. Lett. **46**, 592 (1985).

[16]F. Hottier and J. B. Theeten, J. Cryst. Growth **48**, 644 (1980).

[17]B. Drevillon, Thin Solid Films **130**, 165 (1985).

[18]D. E. Aspnes, Proc. SPIE Int. Soc. Opt. Eng. **276**, 188 (1981).

[19]R. M. A. Azzam and N. M. Bashara, *Ellipsometry and Polarized Light* (North-Holland, Amsterdam, 1977).

[20]A. Mazor, D. J. Srolovitz, P. S. Hagan, and B. G. Bukeit, Phys. Rev. Lett. **60**, 424 (1988).

[21]R. W. Collins and B.-Y. Yang, J. Vac. Sci. Technol. B **7**, 1155 (1989).